EG UK Computer Graphics & Visual Computing (2018)
G. Tam and F. Vidal (Editors)

Groupwise non-rigid image alignment with graph-based initialisation

A. Aal-Yhia[1,2], P. Malcolm[3], O. Akanyeti[1], R. Zwiggelaar[1] and B. Tiddeman[1]

[1]Department of Computer Science, Aberystwyth University, Aberystwyth, *SY*23 3*DB*, UK, {aha10, ota1, rrz, bpt}@aber.ac.uk
[2]Post-Graduate Institute for Accounting & Financial Studies, University of Baghdad, Baghdad, Iraq
[3] Department of Radiology, Norfolk Norwich University Hospital, Norwich *NR*4 7*UY*, UK, paul.malcolm@nnuh.nhs.uk

Abstract

Groupwise image alignment automatically provides non-rigid registration across a set of images. It has found applications in facial image analysis and medical image analysis by automatically generating statistical models of shape and appearance. The main approaches used previously include iterative and graph-based approaches. In iterative approaches, the registration of each image is iteratively updated to minimise an error measure across the set. Various metrics and optimisation strategies have been proposed to achieve this. Graph-based methods perform registration of each pair of images in the set, to form a weighted graph of the "distance" between all the images, and then finds the optimal paths between the most central image and every other image. In this paper, we use a graph-based approach to perform initialisation, which is then refined with an iterative approach. Pairwise registration is performed using demons registration, then shortest paths identified in the resulting graph are used to provide an initial warp for each image by concatenating warps along the path. The warps are refined using an iterative Levenberg-Marquardt minimisation to the mean, based on updating the locations of a small number of points and incorporating a stiffness constraint. This optimisation approach is efficient, has very few free parameters to tune and we show how to tune the few remaining parameters. We compare the combined approach to both the iterative and graph-based approaches used independently. Results demonstrate that the combined method improves the alignment of various datasets, including two face datasets and a difficult medical dataset of prostate MRI images.

CCS Concepts

•***Computing methodologies*** → ***Computer vision; Matching; Image processing;***

1. Introduction

Non-rigid alignment of a group of images is required for many applications such as analysis of face images [CTV*05] and constructing anatomical atlases from medical images [TMT04]. Analysing the structure of the alignment across groups of images can be used for building statistical models of appearance and shape, such as Active Appearance Models (AAMs) [CET01] [MB04] which can then be used for interpreting those and other images. When building such models from large databases, automation is essential for avoiding using manual annotation that is time consuming and prone to error. Using the statistical model in training with a set of images provides a set of deformation fields across this group without manual intervention [CTV*05]. Groupwise registration algorithms are an optimisation problem that is solved by using a suitable minimisation method. Therefore, they require selecting a good initialization algorithm [ZC12].

[JWW*12] used graph-based groupwise image registration by building a directed graph for all image pairs in a dataset and calculated a minimum spanning tree for groupwise registration using the template and the directed paths.

In their work using medical and other images, [HYVD10] used the manifold structure as a way to facilitate registration. The manifold is modelled as a k Nearest Neighbour (kNN) graph based on a pairwise measure between images. Transformation is estimated by using the shortest path between pairs of images and each edge in the path represents a transformation between a pair of (similar) images. They assume a subset of pairwise registration good enough and a single template sufficient. They exploit a manifold learning technique which provides the requested information of neighbourhood for the database images for getting a good estimation of the deformation fields. This estimation is exploited in this paper to do the initialisation of groupwise registration.

In this paper, we combine the graph method of Hamm with a groupwise optimisation which is described in [AYMZT18]. The proposed combination (full method) is compared with the graph only algorithm and the groupwise only algorithm. The groupwise only method builds on the work of [CTP*10] and [SRM09]. It is

DOI: 10.2312/cgvc.20181203

based on using a very small number of control points per iteration and uses an AAM style optimisation [MB04]. More complex warps can be built up over iterations [SRM09] by concatenation [TDR01]. Leave-one-out optimization and alignment to the mean [CTP*10], [SRM09] is used. The use of Levenberg-Marquardt optimisation provides stability and automatic tuning of the damping term.

2. Method

This section describes the algorithmic details of the proposed method that consists of two phases. The first phase is for initialisation of groupwise registration. The initialisation is by constructing a distance graph using pairwise registration of all images in the dataset. The shortest paths between all pairs of images are calculated and used to select the "template" as the image having the smallest sum of shortest paths to all other images. The shortest paths from the template to all other images are calculated for getting the warps from the template to each image along the shortest path. This structure is taken from [HYVD10] with some changes that we have used a different distance metric. In addition, we have concatenated the warps of the images with template shape using [TDR01].

The second phase uses the resulting images and their warps to achieve a groupwise alignment algorithm to update these warps as shown in [AYMZT18]. The following sections describe our method in more detail.

2.1. Graph method for initialization

This section describes the proposed graph method to initialize the groupwise registration. A distance graph is constructed by pairwise registration between all image pairs using the demons algorithm [KS09]. For getting the distance graph, a pixel error term and a smoothness term are computed. The pixel error term measures the error between an obtained image from the registration process (I_i) and a target image (I_j). The smoothness term measures the size of the warp, ignoring the affine components, as shown by the equations 1 and 2:

$$pixel\_error(i,j) = \sqrt{(\frac{1}{N}\sum_y\sum_x (I_i(x,y) - I_j(x,y))^2)} \quad (1)$$

$$smoothness(i,j) = \sqrt{(\frac{1}{N}\sum_y\sum_x u_x^2 + u_y^2)} \quad (2)$$

Where x and y are pixel coordinates in an image, N is the number of pixels, and u_x, u_y are the warp functions resulting from the removal of the affine component of the warp. The affine components (translate, scale, rotate and shear) are removed from the resulting warps by finding the affine registration parameters (a, b, c, d, e, f) that minimize the difference with the given warping function w_x and w_y as shown in equation 3.

$$\chi^2 = \sum_x\sum_y (ax+by+c-w_x(x,y))^2 + (dx+ey+f-w_y(x,y))^2 \quad (3)$$

The distance graph $D(i,j)$ is computed by adding the pixel error term to the smoothness term multiplied by λ as shown in equation 4, where λ controls the contribution between the pixel error term and the smoothness term.

$$D(i,j) = pixel\_error(i,j) + \lambda smoothness(i,j) \quad (4)$$

The Floyd-Warshall algorithm [Ros12], [Cha10] is used to get the shortest paths S between all pairs of vertices in the graph. The template T (geodesic mean) is computed automatically by finding the image with the smallest sum of shortest paths [HYVD10] as shown in equation 5.

$$T = argmin_i \sum_j S(I_i, I_j) \quad (5)$$

Then Dijkstra's algorithm [Dij59] is used to find the shortest paths from the template to all the other images and vice-versa as shown in Figure 1. So, we have the series of indices for the shortest path for each image to the template. At this step, the warps from the template to each image along that path are computed as shown in Figure 2. The warps between the images are concatenated [TDR01] along the path to make a single warp. The original images are interpolated with their concatenated warp fields to obtain the new warped images. These initial aligned training images and their warp fields are used in the next section.

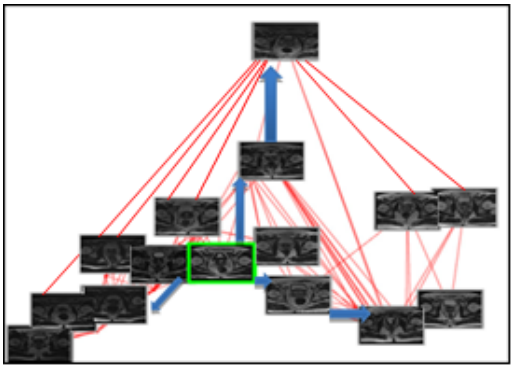

Figure 1: *Finding the shortest paths (highlighted with blue arrows) from the template (highlighted in green) to all other images. Red lines indicate the edges that connect images on the graph.*

2.2. Groupwise registration approach

The resulting images and their warp fields are then used with the groupwise alignment algorithm. We do the whole process in a multiresolution way so that an image starts blurry and gradually gets sharper. The mean of all the warped images is computed to get an average image which is recomputed over iterations. The proposed groupwise registration method proceeds as shown in the Algorithm 1.

In each iteration we aim to minimise an objective function by

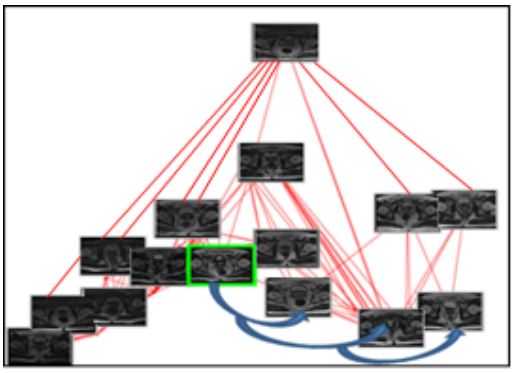

Figure 2: *Warps (highlighted with blue arrows) are computed from the template (highlighted in green) to each image along the shortest path for it. Red lines indicate the edges that connect images on the graph.*

```
input : Pairwise registered images and initial warp functions,
        stiffness parameter for each resolution
output: Updated warps for each image
for resolution from lowest to highest do
    for k iterations do
        Compute average image;
        Calculate new random control points;
        Calculate derivatives of average image (A);
        Calculate A^T A + β D^T K^T K D;
        for each image do
            Warp the current image using the current warp;
            Set up the control points on the average image and
              warped image;
            Find update to the control points using
              Levenberg-Mardquart algorithm;
            Warp using new control points;
            Concatenate the previous and new warps;
        end
    end
end
```

Algorithm 1: Groupwise registration algorithm overview

updating the location of the control points on the target image. The objective function we use is given in vector form by:

$$\chi^2 = \beta(K(w(p+\delta p))+c)^2 + (S + A\delta p - T)^2 \qquad (6)$$

Where β is the stiffness parameter, K is the stiffness matrix that calculates the vector difference between each control point's movement and the average of its neighbours, S is the average image, T is the target image, $w(p+\delta p)$ is the vector of warped control points, $\delta p = \delta p_j$ is the vector of control point location updates, p is the current estimate of their movement, c is the offset vector which is computed using $-k * w(p)$ only of the first iteration, and we have used a first order Taylor series approximation for $S(p+\delta p)$ using the matrix of derivative images A. The stiffness parameter is required to avoid large distortions that may not reduce the error much, particularly in featureless parts of the image. We approximate $w(p+\delta p)$ by its first order Taylor series per control point and derivatives only need to be evaluated at that point. The error function can then be approximated by:

$$\chi^2 = \beta(K(w(p) + D\delta p) + c)^2 + (S + A\delta p - T)^2 \qquad (7)$$

Where D is a block diagonal matrix, with each block a $2x2$ matrix of the derivatives of the warp from the previous iteration at the corresponding point. Taking the derivative of the above with respect to the update parameters and setting the result to zero gives the update equation:

$$2\beta D^T K^T (KD(w(p) + \delta p) + c) + 2A^T (S + A\delta p - T) = 0 \qquad (8)$$

Rearranging gives:

$$(\beta(D^T K^T K D) + A^T A)\delta p = -\beta D^T K^T (Kw(p) + c) - A^T (S - T) \qquad (9)$$

In line with the usual Levenberg-Marquardt procedure, we modify the above equation to vary smoothly between the Gauss Newton version (above) and the gradient descent method, via the inclusion of a damping term:

$$(B + \alpha \operatorname{diag} B)\delta p = -\beta D^T K^T (Kw(p) + c) - A^T (S - T) \qquad (10)$$

Where $B = (\beta(D^T K^T K D) + A^T A)$ and α is the damping term. In each iteration across the set, the (random) control points are fixed, as is the average and its derivatives, and so only involve an update of the matrix according to the damping parameter and inversion of a small matrix. The damping term α is initialized with the value 10 and decreased by a factor of 10 for steps that improve the error. For steps where the error worsens, the damping factor is increased by a factor of 10 and the step is discarded.

The deformation fields are represented by a set of control points that parameterize Thin Plate Splines (TPS) [Boo89]. The grid of control points consists of 25 points. The locations of the control points are changed in random order within 25 areas for the current and average image per iteration across the set.

The partial derivatives of the average with respect to movement of each control point are calculated using a finite difference approximation. For every control point on the average image, the x or y value is modified by δp. The control points without change and the control points with one point changed in x or y are input to a TPS function to create a warp for the image. As a result, the derivative images will be obtained by subtracting the warped image from the average image and the resulting value is divided by δp.

The derivative images ($\delta S^0, \delta S^1, \delta S^2, \ldots, \delta S^N$) are saved as a matrix A. Then, a matrix $A^T A$ is computed by applying the dot product operator between all pairs of derivatives contained in matrix A. The step size δp is varied with the resolution, going from 4, 3, 2 and 1 from lowest to highest respectively. The resolution parameter (r)

controls a Gaussian blurring and its values are selected according to values of the step size (s) by using the formula $r = 2^{s-1}$. So, values of the resolution parameter are with widths 8, 4, 2 and 1 respectively.

We present a simulation method that can be used to tune the stiffness parameter β as described in [AYMZT18]. Our experiments use the control points on three different datasets of face and prostate images and each of them varies in terms of brightness and contrast, and so requires a different value for β. The method we propose creates synthetic images with known update as the ground truth, which can be used to calculate an optimal value for β. In theory, this approach could be used to estimate a unique value for each image pair, but for efficiency we approximate a single value for each dataset.

The synthetic training data is created by applying a small random warp to each target image, according to a set of random control points placed in the same way as for the main update algorithm. To make the problem more closely match the real data, we also apply a histogram equalisation step, based on matching the histogram of the warped target image to another image in the set, selected at random. We assume the previous warp to be the identity (I), so only a small update is needed, hence $D = I$. So, the first term of equation 8 is replaced by $2\beta(K^T K(p+\delta p))$ and the stiffness parameter is estimated from this equation, solved for β in the least-squares sense over a set of synthetic example training images i.e. the following equation is minimised.

$$\chi^2 = \sum_{i \in \Omega} (\beta a_i - b_i)^2 \tag{11}$$

Where $a_i = (K^T K(\delta p_i))$ is the stiffness vector term given by the stiffness matrix and known required update for the i^{th} example, and $b_i = (A_i)^T (S_i + A_i \delta p_i - T_i)$ is the vector corresponding to the image error and derivatives from the i^{th} example. The solution is given by:

$$\beta = \frac{\sum_{i \in \Omega} a_i \cdot b_i}{\sum_{i \in \Omega} a_i \cdot a_i} \tag{12}$$

We estimate a different value of β for each image set and each resolution. The random offset of each control point is limited to twice the step size for that resolution. Example synthetic images are shown in Figure 3.

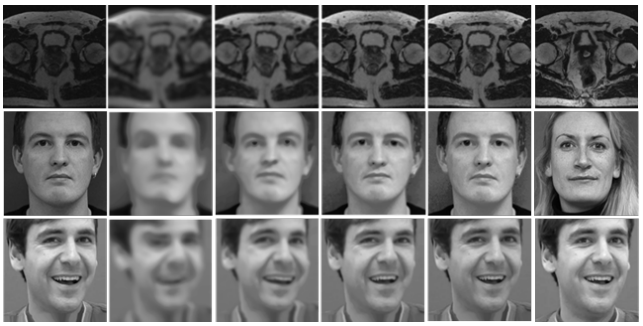

Figure 3: *Examples of the original prostate MRI, IMM, and FGNET images with example synthetic images created using a random warp and offset of each control point. From left to right, the original target image, synthetic images at 4 different scales, with their histograms mapped to a target image, the target image used to provide the histogram.*

2.3. Measuring quality of our model

Datasets: We have tested our model on a set of 100 frames (every 10^{th} frame) of the FGNET "franck" dataset [FgnF04], a set of 37 front-facing faces from the IMM database [NMLS04] and our set of 38 prostate T2-Weighted MRI images from different patients, where every image represents a slice from a patient.

Specificity: We use the specificity measure as described in [CTV*05] to assess our model. By using the aligned images and warps obtained from the groupwise approach, we have used the PCA method to build appearance and shape models. The affine part is removed from the aligned warps before building the shape model. The appearance and shape model distributions are used to construct a set of random images - 1000 images were generated for each dataset. We apply the estimate of the affine transformation obtained from the aligned warps to the original training images to produce the affine registered images. We use the random images and the affine registered images for computing the specificity measure.

Pixels' intensity error: We have calculated the error of the pixels' intensity for evaluating the performance of our model. The errors of the pixel intensities are calculated for the three datasets and three methods by computing the error between the average image and a groupwise registered image.

Feature shapes error: We have calculated the error of feature shapes (either point locations or segmented areas) for evaluating the performance of the model. The error on feature points is performed for PGNET and IMM datasets by using the manual ground truth points which are available publicly [FgnF04], [NMLS04]. The evaluation metric of the errors on feature points used in this study is similar to that described by [CTP*10]. The feature points used for each image are twenty points as shown in Figure 4. The warps fields of the groupwise registered images are used for computing a mean location for each point for all images on the final average image to estimate the true position of the feature points. Then the warp fields are used to project those mean reference points back to each groupwise registered image for comparing them with the actual positions of the ground truth points. For the prostate MRI images we have the location of the prostate annotated by a clinical expert as a region segmentation rather than as feature points. Figure 4 shows an example label image from a prostate image. It is important to note that the prostate region is lacking in clear intensity variations, and so is a particularly challenging region for automatic alignment. We used the Dice overlap to evaluate the results of the prostate images as described in [CTP*10]. The deformation fields of the groupwise registered images are used to warp each segmented prostate image (label image). The resulting warped label images are averaged and thresholded at 0.5, and this average is considered as the ground truth segmentation of the average. This ground truth is used with

each warped label image to compute the Dice overlap for a particular image. Then the mean Dice overlap of all images in T2-MRI dataset is computed.

Statistical analysis: We have used Anova statistical test for analysis the variance differences among the three experiments for each dataset.

Figure 4: *Left to right: example ground truth points used for evaluation of the PGNET dataset, ground truth points used for evaluation of the IMM dataset, and ground truth region segmentation of the prostate used to evaluate the T2-MRI dataset.*

3. Results

3.1. Specificity

The results of the specificity for PGNET dataset are 0.027, 0.028 and 0.034 for the full method, graph only and groupwise only experiments respectively. These results indicate that full method is better than graph only and groupwise only methods. The results of the specificity for IMM dataset are 0.082, 0.091 and 0.099 for full method, graph only and groupwise only experiments respectively. These results indicate a good performance of the full method. The results of the specificity for T2-MRI dataset are 0.107, 0.109 and 0.112 for the full method, graph only and groupwise only experiments respectively. These results indicate that the full method is better than the graph or groupwise methods alone. The results are shown in Figure 5.

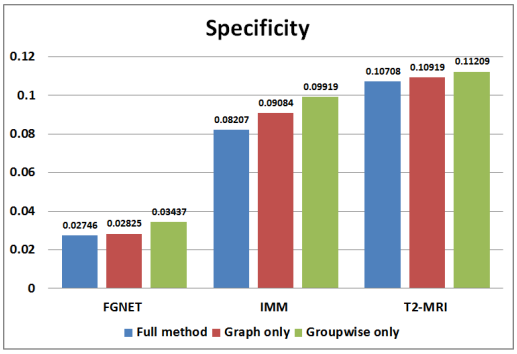

Figure 5: *Results of specificity comparison for full method, graph only and groupwise only experiments according to PGNET, IMM and T2-MRI datasets. The results show a good performance for our method.*

3.2. Pixels' intensity error

For the PGNET dataset, the results of the mean and standard deviation of the intensity error for the three experiments are as follow: full method is 0.0293 (0.0075), graph only is 0.0377 (0.0116) and groupwise only is 0.0407 (0.0110). Figure 6 shows that the full method is significantly different from graph only and groupwise only methods. For the IMM dataset, the results of the mean and standard deviation of the intensity error for the three experiments are as follow: full method is 0.0738 (0.0291), graph only is 0.1030 (0.0372) and groupwise only is 0.0840 (0.0435). Figure 7 shows that the full method is significantly different from graph only method and is better than groupwise only method. For the T2-MRI dataset, the results of the mean and standard deviation of the intensity error for the three experiments are as follow: full method is 0.1117 (0.0237), graph only is 0.1277 (0.0189) and groupwise only is 0.1134 (0.0201). Figure 8 shows that the full method and groupwise only are significantly different from the graph only method.

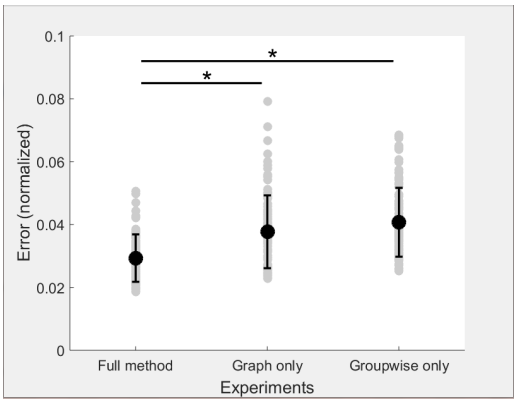

Figure 6: *Shows normalized error of the pixels' intensity of full, graph only and groupwise only methods for the PGNET dataset. * indicates significance at ($p < 0.05$, Anova). Grey filled circles indicate individual values obtained from pairwise image comparisons. Black filled circles and error bar point to the mean and standard deviation, respectively.*

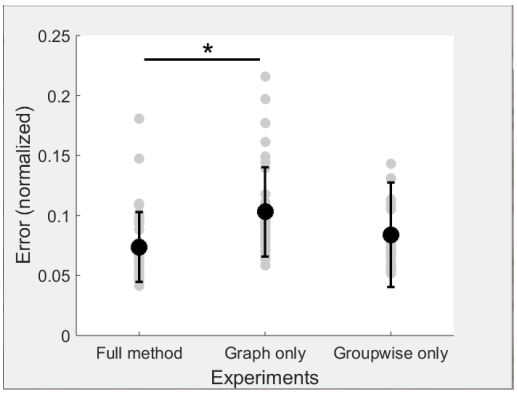

Figure 7: *Shows normalized error of the pixels' intensity of full, graph only and groupwise only methods for the IMM dataset. * indicates significance at ($p < 0.05$, Anova). Grey filled circles indicate individual values obtained from pairwise image comparisons. Black filled circles and error bar point to the mean and standard deviation, respectively.*

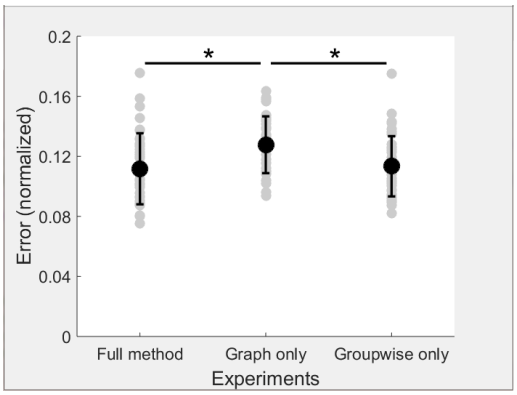

Figure 8: *Shows normalized error of the pixels' intensity of full, graph only and groupwise only methods for the T2-MRI dataset. * indicates significance at ($p < 0.05$, Anova). Grey filled circles indicate individual values obtained from pairwise image comparisons. Black filled circles and error bar point to the mean and standard deviation, respectively.*

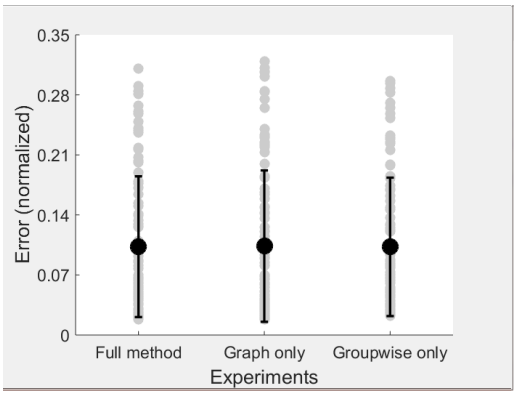

Figure 9: *Shows normalized error of the feature point of full, graph only and groupwise only methods for the PGNET dataset. Grey filled circles indicate individual values obtained from pairwise image comparisons. Black filled circles and error bar point to the mean and standard deviation, respectively.*

Table 1: *The results of the mean Dice overlap for the three experiments on the T2-MRI prostate dataset.*

Experiment name	Mean of Dice overlap
Full method	48.4%
Graph only	47.3%
Groupwise only	40%

3.3. Feature shapes error

We show firstly the results of the error of feature shapes (point locations). For the PGNET dataset, the results of the mean and standard deviation of the point error for the three experiments are as follow: full method is 0.1030 (0.0885), graph only is 0.1037 (0.0919) and groupwise only is 0.1028 (0.0872). Figure 9 shows that groupwise only method is a little bit better than the full method and that both are better than graph only method. For the IMM dataset, the results of the mean and standard deviation of the point error for the three experiments are as follow: full method is 0.3295 (0.2368), graph only is 0.2833 (0.2125) and groupwise only is 0.4089 (0.3327). Figure 10 shows that graph only method is significantly different from the groupwise only method and the full method is better than the groupwise only method.
We show secondly the results of the error of feature shapes (segmented areas). For T2-MRI dataset, the results of the mean Dice overlap for the three experiments are as follow: full method is 0.4843, graph only is 0.4727 and groupwise only is 0.4009. The results demonstrate our model performs better than the others as shown in the Table 1.

Figure 11 shows the evolution of the mean of the full method, graph only and groupwise only methods for PGNET, IMM, and T2-MRI datasets.

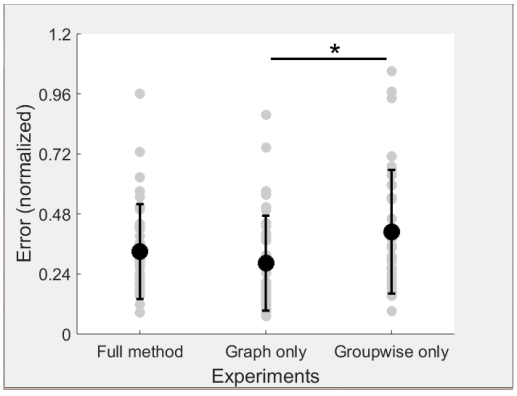

Figure 10: *Shows normalized error of the feature point of full, graph only and groupwise only methods for the IMM dataset. * indicates significance at ($p < 0.05$, Anova). Grey filled circles indicate individual values obtained from pairwise image comparisons. Black filled circles and error bar point to the mean and standard deviation, respectively.*

4. Discussion

The proposed graph-based initialisation is based on the work of Hamm et al. [HYVD10], which is borrowed from the Isomap algorithm. It can approximate the group of images using the shortest path inside a *kNN* graph that connects this group of images.
The pros of the proposed graph-based initialisation are as follows. We can compute the template automatically rather than select one image at random. As our proposed method is based on the structure of the Isomap algorithm, the dataset of images is assumed to be distributed on a low dimensional space that is produced from the manifold learning algorithm. Although some our datasets have small number of images, the results has been shown to demonstrate improved registration compared to the other methods in this paper. Whilst the cons of the proposed method are as follows. Our method

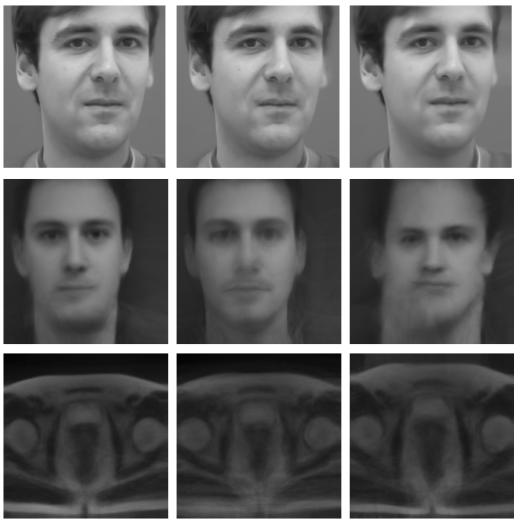

Figure 11: *Evolution of the mean of the three methods and datasets. From left to right: full method, graph only method and groupwise only method. From top to bottom: PGNET, IMM, and T2- MRI datasets.*

has the same limitations as the Isomap algorithm. i.e. the number of samples needed increases exponentially with the intrinsic dimension of the data. Although our algorithm is less dependent on having a very large dataset, due to the use of refinement of the non-rigid registration. We use pairwise registration between every pair of images and that is computationally expensive.

5. Conclusion

In this paper, we combine a graph-based groupwise registration method, based on the work of Hamm et al. [HYVD10] with a groupwise optimisation method ([AYMZT18]) based on the work of Cootes et al. [CTP*10] and Sidorov et al. [SRM09] . The proposed combination (full method) is compared with the graph only algorithm and the groupwise only method. Our model has been tested on three different datasets of faces and medical images and indicates good results, in most cases better than the other two methods. Of the nine evaluations, comprising 3 measurements (specificity, pixel intensity error, and feature based error) on the 3 datasets, the combined method showed an improved performance in 7 of them (all the specificity and intensity measures and the region segmentation feature measure). The two where it performed worse than the other method (in both cases the graph only method) it was not significantly worse at the $p = 0.05$ level. This shows that the combination of a graph-based initialisation approach with a groupwise update of the alignment shows promise for improved unsupervised non-rigid image alignment.

6. Acknowledgements

Ahmad Aal-Yhia thanks Iraqi Ministry of Higher Education and Scientific Research for funding his PhD.

References

[AYMZT18] AAL-YHIA A., MALCOLM P., ZWIGGELAAR R., TIDDEMAN B.: Towards parameter free groupwise non-rigid image alignment. In *International Conference on Computer Graphics, Visualization, Computer Vision and Image Processing* (2018). 1, 2, 4, 7

[Boo89] BOOKSTEIN F.: Principal warps: Thin-plate splines and the decomposition of deformations. *IEEE Trans. Pattern Anal. Machine Intell 11* (1989), 567–585. 3

[CET01] COOTES T., EDWARDS G., TAYLOR C.: Active appearance models. *IEEE Transactions on Pattern Analysis and Machine Intelligence 23*, 6 (2001), 681–685. 1

[Cha10] CHAN T.: More algorithms for all-pairs shortest paths in weighted graphs. *SIAM Journal on Computing 39*, 5 (2010), 2075–2089. 2

[CTP*10] COOTES T., TWINING C., PETROVIĆ V., BABALOLA K., TAYLOR C.: Computing accurate correspondences across groups of images. *IEEE Transactions on Pattern Analysis and Machine Intelligence 32*, 11 (November 2010), 1994–2005. 1, 2, 4, 7

[CTV*05] COOTES T., TWINING C., V.PETROVIC, R.SCHESTOWITZ, TAYLOR C.: Groupwise construction of appearance models using piecewise affine deformations. In *British Machine Vision Conference (BMVC)* (2005), pp. 879–888. 1, 4

[Dij59] DIJKSTRA E.: A note on two problems in connection with graphs. *Numerische Mathematik 1*, 1 (1959), 269–271. 2

[FgnF04] FACE, GESTURE NETWORK (FGNET):. http://www-prima.inrialpes.fr/FGnet/data/01-TalkingFace/talkingface.html, 2004. 4

[HYVD10] HAMM J., YE D., VERMA R., DAVATZIKOS C.: Gram: A framework for geodesic registration on anatomical manifolds. *Medical Image Analysis 14*, 5 (2010), 633–642. 1, 2, 6, 7

[JWW*12] JIA H., WU G., WANG Q., WANG Y., KIM M., SHEN D.: Directed graph based image registration. *Computerized medical imaging and graphics: the official journal of the Computerized Medical Imaging 36*, 2 (2012), 139–151. 1

[KS09] KROON D., SLUMP C.: Mri modalitiy transformation in demon registration. In *IEEE International Symposium on Biomedical Imaging: From Nano to Macro, Boston, MA* (2009). 2

[MB04] MATTHEWS I., BAKER S.: Active appearance models revisited. *International Journal of Computer Vision 60*, 2 (2004), 135–164. 1, 2

[NMLS04] NORDSTRØM M., M. LARSEN J. S., STEGMANN M.: The imm face database - an annotated dataset of 240 face images. *Technical report, Technical University of Denmark* (2004). 4

[Ros12] ROSEN K.: *Discrete Mathematics and Its Applications, 7th Edition*. McGraw-Hill, New York, 2012. 2

[SRM09] SIDOROV K., RICHMOND S., MARSHALL A.: An efficient stochastic approach to groupwise non-rigid image registration. In *IEEE Computer Vision and Pattern Recognition* (2009), pp. 2208–2213. 1, 2, 7

[TDR01] TIDDEMAN B., DUFFY N., RABEY G.: A general method for overlap control in image warping. *Computers and Graphics 25*, 1 (2001), 59–66. 2

[TMT04] TWINING C., MARSLAND S., TAYLOR C.: Groupwise non-rigid registration: The minimum description length approach. In *British Machine Vision Conference (BMVC)* (2004), pp. 417–426. 1

[ZC12] ZHANG P., COOTES T.: Automatic construction of parts+geometry models for initializing groupwise registration. *IEEE Transactions on Medical Imaging 31*, 2 (February 2012), 341–358. 1